JOC The Journal of Organic Chemistry

Article

pubs.acs.org/joc

Capture of an Elusive Nitrile Ylide as an Intermediate in Isoxazole−Oxazole Photoisomerization

Cláudio M. Nunes,* Igor Reva,* and Rui Fausto

Department of Chemistry, University of Coimbra, P-3004-535 Coimbra, Portugal

Supporting Information

ABSTRACT: The unimolecular photochemistry of 3,5-dimethylisoxazole (**1**) induced by a narrow-band tunable UV laser was studied using low-temperature matrix isolation coupled with infrared spectroscopy. Monomers of **1** were isolated in argon matrices at 15 K and characterized spectroscopically. Irradiation of matrix-isolated **1** at λ = 222 nm (near its absorption maximum) led to the corresponding 2*H*-azirine **3** and ketenimine **6** as primary photoproducts and also to nitrile ylide **4** and 2,5-dimethyloxazole (**5**). The photoproducts were identified (i) by comparison with infrared spectra of authentic matrix-isolated samples of **3** and **5** and (ii) using additional irradiations at longer wavelengths (where **1** does not react) which induce selective photoisomerizations of **4** and **6**. In particular, irradiation with λ = 340 nm led to the unequivocal identification of the nitrile ylide *anti*-**4**, which was transformed into oxazole **5**. The details of the 1,5-electrocyclization of the carbonyl nitrile ylide **4** and its structural nature (propargyl-like versus allene-like geometry) were also characterized using theoretical calculations. Thus, the elusive carbonyl nitrile ylide **4** was captured and characterized for the first time as an intermediate in the isoxazole−oxazole photoisomerization.

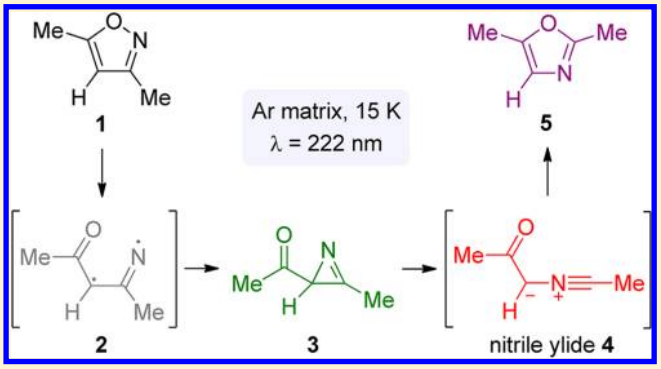

INTRODUCTION

Isoxazoles are five-membered heterocyclic compounds with important applications in areas such as pharmaceuticals, agrochemistry, molecular electronics, corrosion inhibitors, liquid crystalline materials, and others.[1−3] Isoxazoles are also important building blocks in organic synthesis. Their aromatic character gives enough stabilization to allow the manipulation of their substituents, and on the other hand, their weak N−O bond can be easily cleaved under different conditions to give functionalized compounds.[1−3]

Under photochemical conditions isoxazoles rearrange to oxazoles via 2*H*-azirine intermediates, which show a remarkable wavelength-dependent photochemistry.[4−6] This fascinating photochemical transformation was first reported by Ullman and Singh in 1966.[4] Afterward, several other studies were carried out and isoxazole−oxazole isomerization has been established as the most common pathway in isoxazole photochemistry.[7−23] From a mechanistic point of view, the first step of this photoisomerization reaction has been suggested to occur through cleavage of the N−O bond of isoxazole **I** with the generation of a diradical, the vinyl nitrene type reactive intermediate **II**, which rapidly collapses to give the 2*H*-azirine **III** (Scheme 1). Then the 2*H*-azirine **III** can undergo C−C bond cleavage to generate a zwitterionic species, the nitrile ylide type reactive intermediate **IV**, which quickly isomerizes to oxazole **V**.

According to an early theoretical study performed for the isoxazole−oxazole photoisomerization, the existence of vinyl nitrene **II** and nitrile ylide **IV** reactive intermediates is not required.[24] At the MO-CI (STO-3G) ab initio level, the photorearrangement of isoxazole **I** to 2*H*-azirine **III** was theoretically found to occur in a concerted manner through the lowest singlet excited state (S_1). The excitation of 2*H*-azirine **III** to the S_2 excited singlet state induces isomerization to oxazole **V** without any intermediate involved.[24] However, recently we have shown that vinyl nitrenes should play a central role in isoxazole thermal reactivity and also that nitrile ylides should be intermediates in the isomerization of 2*H*-azirines **III** to oxazoles **V**.[25] Nevertheless, concerning the mechanism of isoxazole thermal or photochemical reactivity, until now the postulated reactive intermediates species involved, i.e. the vinyl nitrene **II** and the nitrile ylide **IV**, have escaped from direct experimental identification and their existence still remains to be proved.[26]

In a previous paper,[27] we investigated the photochemistry of the parent isoxazole and found surprisingly no indication of isomerization to oxazole. Instead, we observed the formation of nitriles via the corresponding ketenimine, which was established to be a key intermediate in that reaction. According to the mechanistic model proposed, it is conceivable that the nitrile formation will take place preferentially in the case of the photochemistry of 3-unsubstituted isoxazoles.

Received: July 18, 2013
Published: September 27, 2013

Scheme 1. Photochemical Isomerization of Isoxazoles I to Oxazoles V via 2*H*-Azirines III

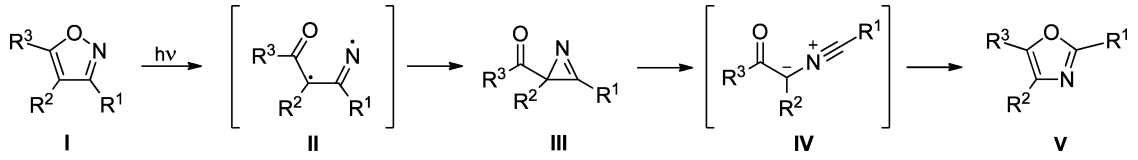

Herein, we report on the photochemistry of 3,5-dimethylisoxazole (**1**, $R^1 = R^3 = Me$, $R^2 = H$; see Scheme 1). In this study we took advantage of a combination of narrow-band tunable UV laser irradiation and low-temperature matrix isolation coupled with infrared spectroscopy, used as experimental techniques. As a result, for the first time, it was possible to capture and identify the elusive nitrile ylide reactive intermediate in the isoxazole−oxazole photoisomerization.

RESULTS AND DISCUSSION

IR Spectrum of Matrix-Isolated 3,5-Dimethylisoxazole. The experimental FTIR spectrum of monomeric 3,5-dimethylisoxazole (**1**) isolated in an argon matrix at 15 K and the simulated theoretical IR spectrum are shown in Figure 1.

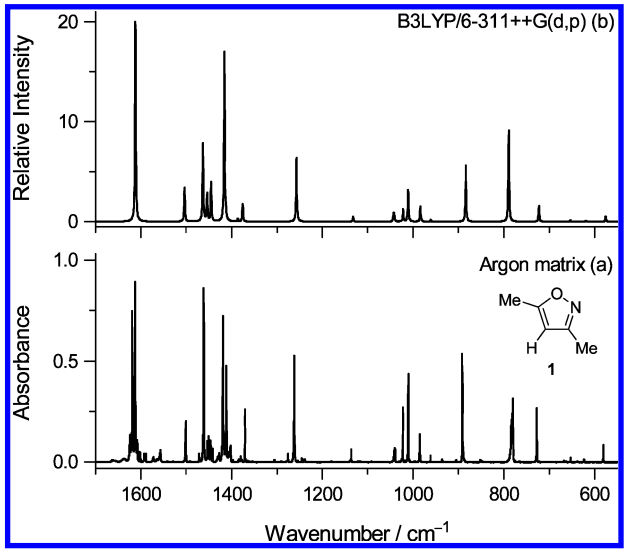

Figure 1. (a) Experimental FTIR spectrum of 3,5-dimethylisoxazole (**1**) isolated in an argon matrix at 15 K. (b) IR spectrum of **1** simulated at the B3LYP/6-311++G(d,p) level of theory (for details, see the Experimental Section).

The intense bands observed at ∼1616 and ∼1415 cm^{-1} in the experimental IR spectrum of **1** exhibit a site-splitting effect. Such an effect results from the fact that the rigid matrix accommodates the guest molecules in different local environments that may present slightly different physicochemical properties. The scaling factor of 0.980 used to correct the calculated frequencies was obtained from a least-squares linear fit of the experimental versus calculated frequencies in the fingerprint region of the IR spectrum (see the Supporting Information, Figure S1). The assignment of the experimental IR spectrum of **1** isolated in an argon matrix, together with the calculated IR spectrum at the B3LYP level, and the results of normal coordinate analysis are presented in Table S1 (Supporting Information). The fact that the density functional theory B3LYP method provides an accurate estimation of vibrational frequencies of **1** gives us additional confidence to use it in the analysis of the experimental IR spectra obtained in the photochemistry study.

Photochemistry of 3,5-Dimethylisoxazole at λ = 222 nm. The photochemistry of 3,5-dimethylisoxazole (**1**) isolated in an argon matrix was induced using narrow-band UV laser light tuned at λ = 222 nm. This wavelength is the lowest available in our laser system, and also, it is close enough to the absorption maximum of **1** (UV-vis (ACN) λ_{max} ∼215 nm, $\varepsilon \approx$ 5500 $dm^3\ mol^{-1}\ cm^{-1}$). Under these conditions, two types of irradiation experiments were carried out: using either shorter (a few seconds) or longer (several minutes) irradiation times. The changes in the samples were followed by infrared spectroscopy after each irradiation.

Figure 2a presents the results of a total irradiation time of 1 min, in which about 2% of **1** was consumed and two photoproducts **A** and **B** were generated. Figure 2b presents the results of a total irradiation time of 80 min, in which about 46% of **1** was consumed and, in addition to **A** and **B**, photoproduct **C** was observed in a considerable amount. The progress of the photochemistry of **1** from 0 to 180 s is shown in Figure S3 (Supporting Information), in the 2150−1630 cm^{-1} region, where the most characteristic bands of the photoproducts appear. The kinetics of the formation of photoproducts shows two relevant facts: (i) initial stage irradiations, i.e. from 0 to 60 s (total time), indicate that photoproducts **A** and **B** are formed simultaneously and that only they appear at the very beginning of the photochemistry; (ii) prolonged irradiations, i.e. from 60 to 180 s (total time), allow identification of another photoproduct, labeled as **C**.

By comparison of the results of short and longer irradiation times (parts a and b of Figure 2), it is evident that for longer irradiation times the ratio between photoproducts **A** and **B** decreases (and therefore **A** and **B** are different species). The data also show the accumulation of photoproduct **C** for longer irradiation times, which is manifested by an increase in the **C**:**A** or **C**:**B** ratio in IR spectra. Finally, the observation of photoproducts labeled as **X** after the formation of the photoproducts **A**−**C**, and after prolonged irradiation, should also be mentioned. These probably result from photodecomposition and will not be discussed here.

Identification of 3,5-Dimethylisoxazole Photoisomerization Products A−C. As shown before, by monitoring IR spectra during a series of irradiations of 3,5-dimethylisoxazole (**1**) (at λ = 222 nm), it was possible to determine the formation of two primary photoproducts, **A** and **B**, and a secondary product, **C**. In this section, we will present the identification of these photoproducts with the aid of IR spectra of authentic samples or with the aid of subsequent irradiation experiments using longer wavelengths: i.e., under conditions where **1** is unreactive but its photoproducts can be transformed.

*Identification of Photoproduct **A**.* For photoproduct **A** the most distinctive band appears at 1713 cm^{-1}, a characteristic region for ν(C═O) vibrations. With this information, 2-acetyl-3-methyl-2*H*-azirine (**3**) arises as a possible candidate for photoproduct **A**, also because it is known that the photo-

dx.doi.org/10.1021/jo4015672 | J. Org. Chem. 2013, 78, 10657−10665

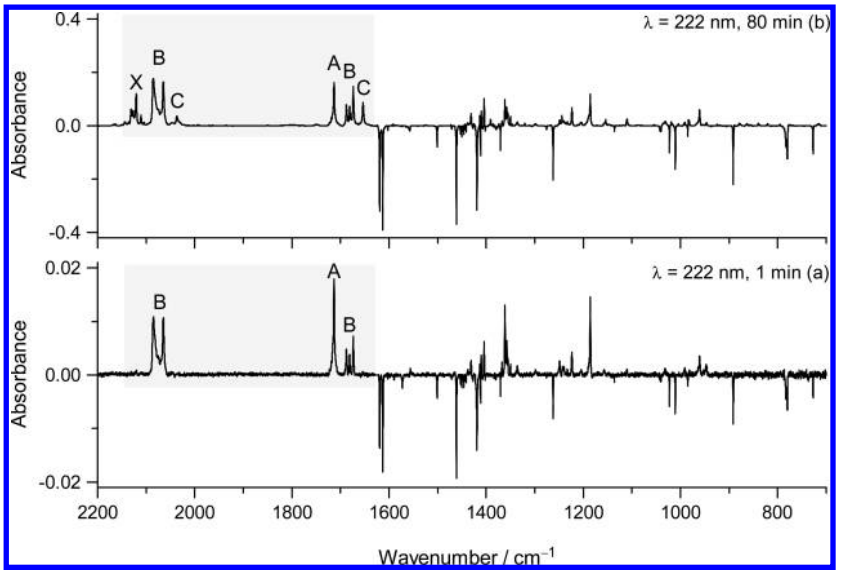

Figure 2. Experimental difference IR spectra obtained as the spectrum after UV irradiation at λ = 222 nm of **1** in an argon matrix minus the spectrum of the sample before irradiation. Total exposition of the samples to UV light: (a) total irradiation time of 1 min; (b) total irradiation time of 80 min. The rectangle in the 2150−1630 cm^{-1} region (specified with a gray background) indicates where the most characteristic bands due to photoisomerization products (labeled as **A**−**C**) appear (see text). Monomeric water bands (at 1624 and 1608 cm^{-1}) were removed from spectra for clarity.[28]

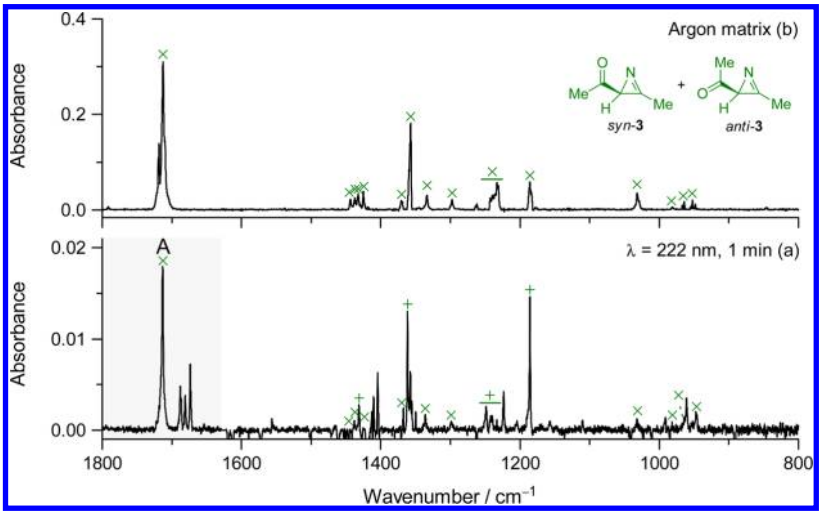

Figure 3. (a) Experimental IR spectrum of photoproducts of **1** in an argon matrix obtained after 1 min of UV irradiation at λ = 222 nm (see also Figure 2a). (b) Experimental IR spectrum of authentic 2-acetyl-3-methyl-2*H*-azirine (**3**) isolated in an argon matrix in a separate experiment.[25] The cross symbol (×) designates the bands of photoproduct **A** assigned to **3**. The plus sign symbol (+) indicates bands due to photoproduct **A** which also have contribution due to photoproduct **B**.

chemistry of **1** in solution leads to **3**, though with a low yield.[16] In fact, as shown in Figure 3, where the experimental IR spectrum of photoproducts of **1** in an argon matrix (λ = 222 nm; 1 min) is compared with the IR spectrum of an authentic **3** isolated in an argon matrix in a separate experiment,[25] the identification of photoproduct **A** as the 2*H*-azirine **3** is unequivocal. The data on experimental and B3LYP calculated IR spectra of 2-acetyl-3-methyl-2*H*-azirine (**3**) are given in Table S3 (Supporting Information).

A comparison of the spectrum of **3** in Figure 3b and the spectrum of photoproduct **A** in Figure 3a shows some differences in the intensities of the IR bands, which arise probably due to a different conformer ratio. Calculations at the B3LYP/6-311++G(d,p) level indicate that the acetyl moiety in 2-acetyl-3-methyl-2*H*-azirine (**3**) adopts syn and anti orientations, with the syn more stable by only about 0.15 kJ mol^{-1} (see Figure S4, Supporting Information). The *syn*-**3**:*anti*-**3** population ratio in the gas-phase equilibrium at room temperature, estimated using the Boltzmann distribution, is about 52:48. This ratio is expected to be trapped in the matrix of **3** prepared using an authentic sample evaporated at room temperature (shown in Figure 3b). However, the ratio *syn*-**3**:*anti*-**3** produced by in situ irradiation of **1** isolated in an argon matrix (the photoproduct **A** shown in Figure 3a) could be different due to distinct experimental conditions.

Identification of Photoproduct ***B***. The most characteristic bands of photoproduct **B** appear at 2085 and 2064 cm^{-1}, spectral region where ketenimines ($R_2C{=}C{=}NR$) generally absorb strongly,[25,29] and between 1690 and 1670 cm^{-1}. These absorptions suggest that 3-acetyl-*N*-methylketenimine (**6**) is a

dx.doi.org/10.1021/jo4015672 | J. Org. Chem. 2013, 78, 10657−10665

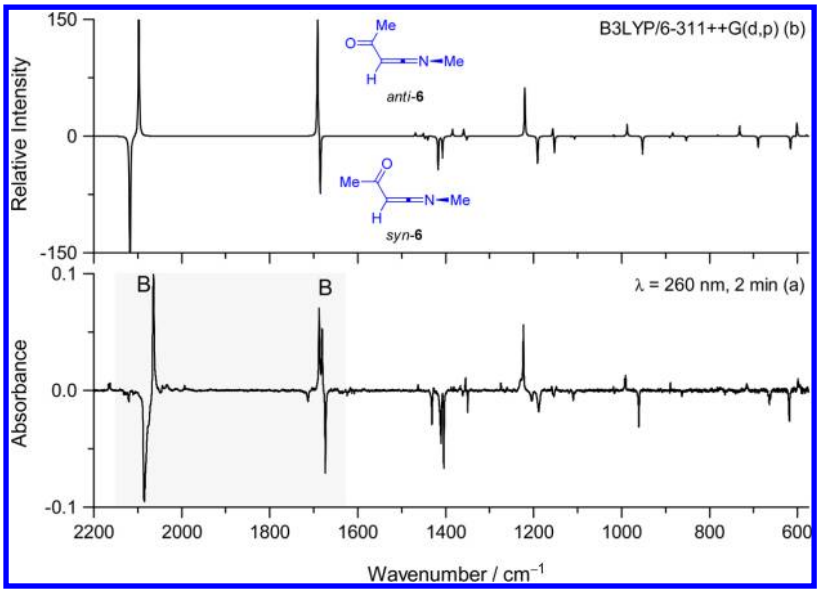

Figure 4. (a) Experimental difference IR spectrum showing changes in the spectrum of photoproduct **B** after 2 min of UV irradiation at λ = 260 nm (after irradiations at 222 nm and at 340 nm). Growing bands are displayed upward. (b) IR spectrum simulated at the B3LYP/6-311++G(d,p) level considering the consumption of *syn*-3-acetyl-*N*-methylketenimine (*syn*-**6**) and the production of *anti*-3-acetyl-*N*-methylketenimine (*anti*-**6**).

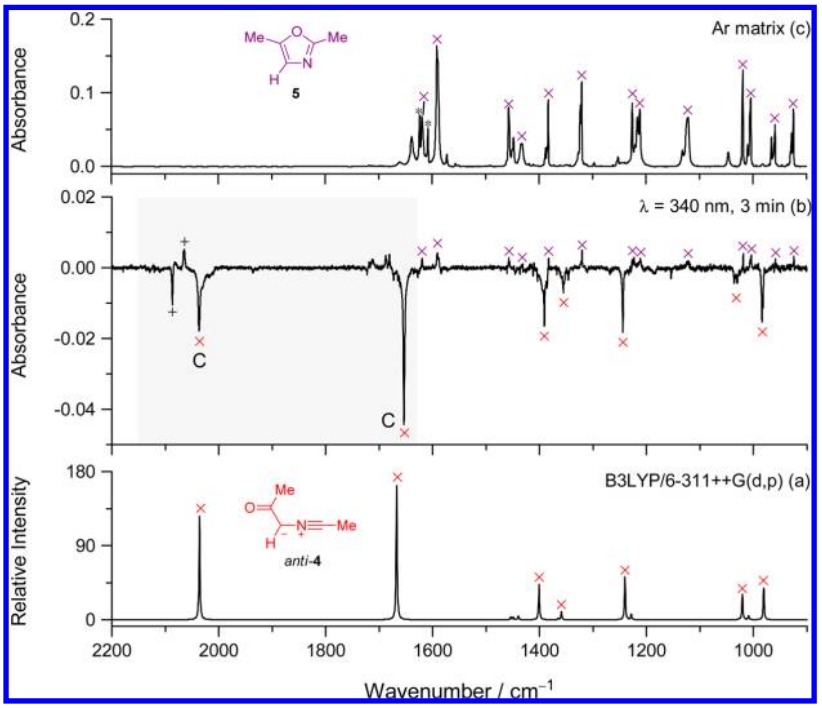

Figure 5. (a) IR spectrum of nitrile ylide *anti*-**4** simulated at the B3LYP/6-311++G(d,p) level. (b) Experimental difference IR spectrum showing changes after 3 min of UV irradiation at λ = 340 nm (subsequent to 80 min of irradiation at λ = 222 nm). Growing bands are displayed upward. The violet crosses (×) designate the bands formed at the expense of **C** and assigned to 2,5-dimethyloxazole (**5**) (positive bands). The red crosses (×) designate the bands of **C** assigned to *anti*-**4** (negative bands). The plus signs (+) indicate bands due to photoproduct **B**, as assigned in Figure 4. (c) Experimental IR spectrum of authentic 2,5-dimethyloxazole (**5**) isolated in an argon matrix in a separate experiment.[25] The asterisks (*) indicate bands of monomeric water.

possible candidate for photoproduct **B**. Indeed, **6**, generated from the reaction of 2,5-dimethylisoxazolium iodine with triethylamine at −77 °C, was characterized by an IR absorption band at 2075 cm^{-1},[15] which agrees well with the mean frequency of the two bands of **B** observed in this region.

The definitive assignment of photoproduct **B** to ketenimine **6** was established in this study on the basis of results of additional irradiations performed on the photolyzed matrix of **1**. After the isoxazole **1** was irradiated at λ = 222 nm in an argon matrix for 80 min (Figure 2b), further irradiations were performed using longer wavelengths to investigate only the photochemistry of photoproducts of **1**. Thus, after the consumption of photoproduct **C** by irradiations in the 340 nm region (as presented below), it was observed that subsequent irradiations at 260 nm selectively induce changes in photoproduct **B**. As shown in Figure 4a, irradiations at 260

dx.doi.org/10.1021/jo4015672 | J. Org. Chem. 2013, 78, 10657−10665

nm result in redistribution of intensities within the bands of photoproduct **B**, which is consistent with the possibility of photoisomerization. At the B3LYP/6-311++G(d,p) level, ketenimine **6** was found to adopt two conformations, *syn*-**6** and *anti*-**6**, which are characterized by different relative orientations of the acetyl moiety and approximately the same energy (see Figure S5, Supporting Information). Indeed, as shown in Figure 4, the theoretical difference IR spectrum simulating the quantitative isomerization *syn*-**6** → *anti*-**6** demonstrates an excellent agreement with the experimental difference IR spectrum.

For example, the decreasing bands at 2085 and 1674 cm^{-1} match well with frequencies of the ν_{as}(C═C═N) and ν(C═O) vibrations of *syn*-**6**, calculated at 2118 and 1685 cm^{-1}, respectively. On the other hand, the increasing bands at 2064 and 1688/1681 cm^{-1} show a good correlation with the ν_{as}(C═C═N) and ν(C═O) frequencies of *anti*-**6**, calculated at 2098 and 1691 cm^{-1}, respectively. As presented in Table S4 (Supporting Information), these data clearly reveal the photoisomerization of **B** induced by irradiation at λ = 260 nm, the unequivocal identification of photoproduct **B** as 3-acetyl-*N*-methylketenimine (**6**), and the comprehensive assignment of the IR bands of *syn*-**6** and *anti*-**6** conformers.

Identification of Photoproduct **C**. As mentioned before, **C** appears as a secondary photoproduct in the photochemistry of 3,5-dimethylisoxazole (**1**) at λ = 222 nm and then plausibly results from photochemistry of **A** or **B**. Interestingly, after 80 min of irradiation of isoxazole **1** at λ = 222 nm (Figure 2b), it was found that photoproduct **C** was consumed selectively by subsequent irradiation at λ = 340 nm. As shown in Figure 5b, several new low-intensity bands emerge in the IR spectrum concomitant with the consumption of product **C**. A comparison of these new bands with the experimental IR spectrum of authentic 2,5-dimethyloxazole (**5**) isolated in an argon matrix (see Figure 5c) clearly establishes that irradiation at λ = 340 nm transforms product **C** into **5**. Some traces of **5** were also detected in the spectrum obtained after irradiation of isoxazole **1** (λ = 222 nm, 80 min). The experimental and calculated IR spectra of **5** are given in Table S5 (Supporting Information; note that all infrared intensities of **5** are intrinsically very low).

From a mechanistic point of view, the last step of the isoxazole−oxazole photoisomerization might occur through a reactive nitrile ylide intermediate, which should be formed by C−C bond cleavage of the 2*H*-azirine (see Scheme 1). In fact, as shown in Figure 5, the secondary photoproduct **C**, captured in the photochemistry of matrix-isolated isoxazole **1**, is undoubtedly assigned to the nitrile ylide *anti*-**4** on the basis of an excellent correspondence between the calculation and the experiment. For example, the most prominent infrared bands of nitrile ylide appear at 2037 and 1654 cm^{-1} and can be readily assigned to the ν_{as}(C═N═C) and ν(C═O) of *anti*-**4**, calculated to appear at 2036 and 1667 cm^{-1}, respectively. The absence of the *syn*-**4** form was confirmed by comparison of absorptions of photoproducts with calculated IR spectra of *syn*-**4** (see Figure S6, Supporting Information). A comprehensive assignment of the experimental spectrum of **C** to the calculated spectrum of nitrile ylide *anti*-**4** is presented in Table 1.

Mechanistic Discussion of the Photochemistry of 3,5-Dimethylisoxazole. A summary of the experimental results and the mechanistic proposal for the photochemistry of 3,5-dimethylisoxazole (**1**) are presented in Scheme 2. Irradiation experiments of **1** at 222 nm, near its absorption maximum, led to the formation of 2*H*-azirine **3** and ketenimine **6** as primary photoproducts and also to nitrile ylide **4** and oxazole **5**. It is likely that the first step in the photochemistry of **1** involves N−O bond cleavage with the formation of the very reactive vinyl nitrene **2**.[25,27] However, no indications of this intermediate were obtained, even when experiments were performed in nitrogen matrices at 12 K.[30] Although the existence of the vinyl nitrene intermediate **2** remains to be proven, the simultaneous appearance of **3** and **6** during the first seconds of irradiation of **1** suggests the participation of **2** as a key intermediate. In this mechanism, the formation of **2** is followed by its rapid isomerization by two competitive paths: (i) decay to 2*H*-azirine **3** (Scheme 2, green) and (ii) a [1,2]-methyl shift to form ketenimine **6** (Scheme 2, blue).

In order to investigate if two different electronic configurations of **2**, the triplet ground state and the open shell singlet excited state, are each independently responsible for the formation of **3** or **6**, the photochemistry of **1** was also studied in xenon matrices. The heavy-atom xenon matrix might favor the path involving the triplet manifold[31,32] of vinyl nitrene **2**. Nevertheless, the results obtained in xenon matrices did not show significant differences from those obtained in argon matrices.

As already mentioned, upon irradiation experiments at λ = 222 nm, performed on matrix-isolated isoxazole **1**, a series of additional laser irradiations was carried out at longer wavelengths where **1** does not absorb, but its photoproducts do react. These additional irradiations allowed inducing selective transformations in some of photoproducts of **1** and acquire important information about their structures. The irradiation at λ = 260 nm (performed after irradiation at λ = 340 nm) led to

Table 1. Experimental FTIR Spectrum of the Photoproduct C and Selected Vibrational Frequencies and Infrared Intensities of Nitrile Ylide *anti*-4 Calculated at the B3LYP/6-311++G(d,p) Level[a]

Ar matrix (15 K)		calculated		
ν/cm^{-1}	I[b]	ν/cm^{-1}	I[c]	approximate assignment[d]
2037	s	2036	395.6	ν_{as}(CNC)
1654	s	1667	543.1	ν(C═O)
1446	?	1454	10.7	$\delta_{as}(CH_3)'_{nitrile}$
		1450	9.8	$\delta_{as}(CH_3)''_{carbonyl}$
1437	?	1440	5.5	$\delta_{as}(CH_3)'_{carbonyl}$
		1440	9.8	$\delta_{as}(CH_3)''_{nitrile}$
1391	s	1401	134.6	ν_s(CNC) + δ(NCH)
		1365	4.1	$\delta_s(CH_3)_{nitrile}$
1355	m	1359	31.8	$\delta_s(CH_3)_{carbonyl}$
1244	s	1240	166.1	δ(NCH) − ν(CC)
1233	?	1228	20.4	δ(NCH) + ν(CC) − ν_s(CNC)
		1027	1.5	$\gamma'(CH_3)_{nitrile}$ + $\gamma'(CH_3)_{carbonyl}$
1036/1031	m	1021	100.5	$\gamma''(CH_3)_{nitrile}$
1026	vw	1009	15.7	$\gamma'(CH_3)_{nitrile}$ − $\gamma'(CH_3)_{carbonyl}$
984/982	s	981	124.5	$\gamma''(CH_3)_{carbonyl}$
879/877	w	874	21.3	$\nu(CC)_{nitrile}$
777	vw	781	8.8	$\nu(CC)_{carbonyl}$
741	w	717	38.9	γ(CH)

[a]Photoproduct **C** (same as nitrile ylide **4**) was generated during the photochemistry of isoxazole **1** at 222 nm. [b]Experimental intensities are presented in qualitative terms. Abbreviations: s, strong; m, medium; w, weak; vw, very weak. [c]Calculated intensities (I) are given in km mol^{-1}. The calculated B3LYP/6-311++G(d,p) frequencies were scaled by 0.980. [d]Legend: ν, stretching; δ, bending; γ, rocking; +, in syn phase; −, in anti phase; s, symmetric; as, antisymmetric,

dx.doi.org/10.1021/jo4015672 | J. Org. Chem. 2013, 78, 10657−10665

Scheme 2. Summary of the Experimental Observations and the Mechanism for Photochemistry of 3,5-Dimethylisoxazole 1 Isolated in a Low-Temperature Argon Matrix

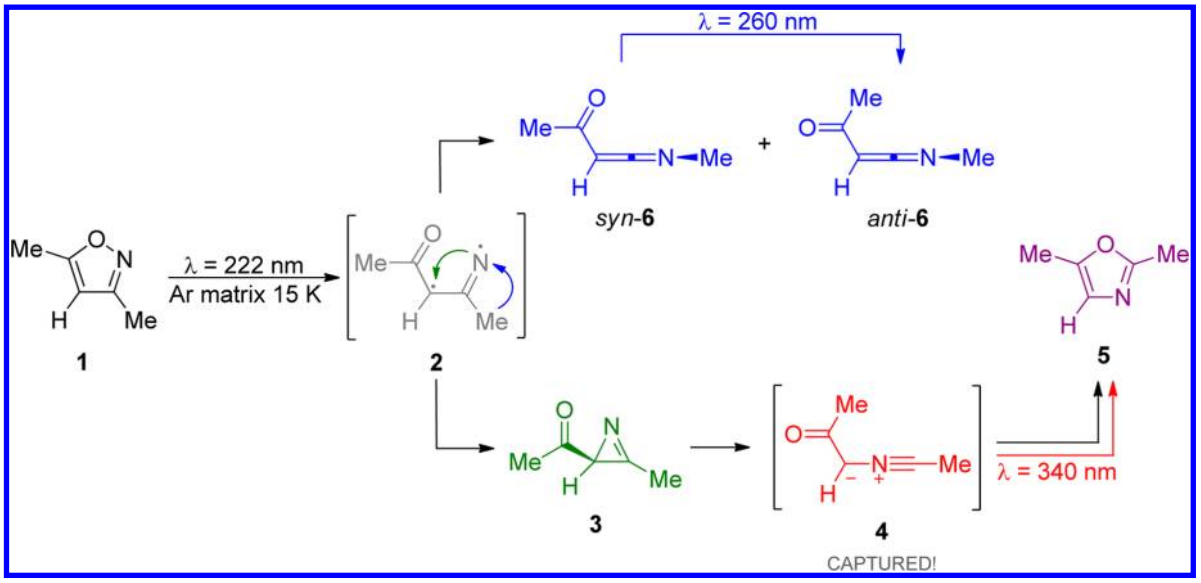

photoisomerization of 3-acetyl-*N*-methylketenimine (**6**). Starting from an approximately equivalent ratio of *syn*-**6** and *anti*-**6** conformers, trapped in the samples upon irradiation of isoxazole **1** at λ = 222 nm, the irradiation at λ = 260 nm induced photoisomerization of *syn*-**6** to *anti*-**6** by intramolecular rotation of the acetyl moiety. This observation could be interpreted as a wavelength-dependent photochemical equilibrium; i.e. the photoequilibrium was strongly shifted toward *anti*-**6** for UV irradiations at 260 nm, whereas *syn*-**6** and *anti*-**6** are in similar amounts in the photoequilibrium after initial irradiations at λ = 222 nm. UV-induced conformational isomerization of the acetyl group has been reported for some matrix-isolated molecules such as hydroxyacetophenone[33] and acetylketene,[34] the latter being structurally very similar to **6**. A wavelength-dependent photochemical equilibrium was also identified in some syn−anti photoisomerizations.[35]

However, the most important result was obtained when the photoproducts of isoxazole **1** were irradiated at λ = 340 nm. This led to the transformation of a secondary photoproduct (initially designated as **C**) and then to its unequivocal identification as being the elusive nitrile ylide *anti*-**4**. The product that results from the photochemistry of *anti*-**4** was reliably identified as 2,5-dimethyloxazole (**5**). Traces of **5** were also detected after irradiation **1** at λ = 222 nm over 80 min. It could be expected that, for extended irradiations of **1**, oxazole **5** would accumulate in the sample as the end product, according to the mechanistic rationalization presented in Scheme 2.

Nature of Nitrile Ylide 4 as an Intermediate in Isoxazole−Oxazole Photoisomerization. The nitrile ylides are species with a CNC framework containing six electrons in π and n orbitals.[36] Typically, due to their high reactivity, nitrile ylides are classified as elusive reactive intermediate species.[37] Therefore, it not surprising that most of the experimental information about the molecular structure of nitrile ylides has been acquired by low-temperature matrix isolation and IR spectroscopy.[38] Nevertheless, to date, only a few acyclic nitrile ylides have been captured and studied using this experimental approach.[29,39−44]

To the best of our knowledge, a carbonyl nitrile ylide reactive intermediate postulated for the isoxazole−oxazole photoisomerization was isolated here and characterized for the first time. The conjugation of the carbonyl group with the nitrile ylide allows for the possibility of an especially facile intramolecular 1,5-electrocyclization, which makes it distinct from all the nitrile ylides so far reported experimentally and even more difficult to observe. The 1,5-electrocyclization reaction to oxazole occurs via a planar or nearly planar nonrotatory transition state involving the in-plane attack of the lone pair of the oxygen carbonyl atom.[45] However, only the nitrile ylide *syn*-**4** is perfectly aligned to provide the possibility of cyclization and must be the precursor of oxazole **5**. *anti*-**4** lacks such a geometric alignment, and precisely this conformer of the nitrile ylide **4** was captured in the matrix and identified in the current work. By analogy with photoproduct 3-acetyl-*N*-methylketenimine (**6**), it could be anticipated that UV irradiation of the matrices induces conformational isomerization also in nitrile ylide **4**.[46] Thus, according to our interpretation, the observed transformation of *anti*-**4** to oxazole **5** must have occurred via the *syn*-**4** intermediate, which has a very low energy barrier toward 1,5-electrocyclization and thus is more difficult to capture. Indeed, the calculated potential energy surface connecting *anti*-**4**, *syn*-**4**, and **5** corroborates our hypothesis (see Figure 6).

The calculated potential energy barrier separating the nitrile ylide *syn*-**4** from the much more stable oxazole **5** is only 10 kJ mol^{-1}. Low barriers can be easily overcome at 15 K in cryogenic matrices by the effect known as conformational cooling.[47,48] Indeed, if the considered molecules are formed in matrices during UV-induced isomerization, they must have an excess of vibrational energy and their thermal relaxation over such low barriers should become even easier. That is why *syn*-**4**, when formed, should instantly collapse to **5**. On the other hand, the *anti*-**4** conformer is not aligned regarding isomerization toward **5**, and the pathway from *anti*-**4** to **5** should go across the *syn*-**4** intermediate. Therefore, the effective barrier between *anti*-**4** and *syn*-**4** is the barrier which stabilizes *anti*-**4** in the matrices. It is equal to 54.5 kJ mol^{-1}, according to the B3LYP/6-311++G(d,p) calculation (see Figure 6). Thus, when *anti*-**4** is produced, such a barrier is high enough to prevent thermal relaxation and allow its capture in the matrix.

dx.doi.org/10.1021/jo4015672 | J. Org. Chem. 2013, 78, 10657−10665

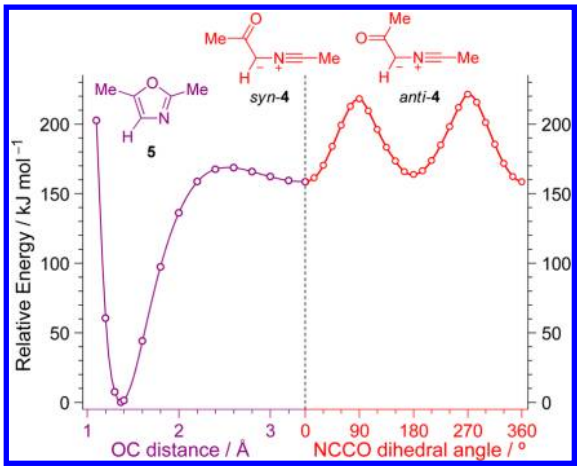

Figure 6. Relaxed potential energy profiles for (right, red) the intramolecular rotation of the acetyl group in nitrile ylide **4** around the NCCO dihedral angle and (left, purple) the ring-contraction from nitrile ylide *syn*-**4** to 2,5-dimethyloxazole (**5**) as a function of the OC distance. The energy of **5** was chosen as the relative zero. Both scans were carried out at the B3LYP/6-311++G(d,p) level of theory.

Finally, it appears instructive to us to comment on the structure of nitrile ylides. It is known that nitrile ylides can be represented by two different resonance structures, propargyl-like and allene-like (Scheme 3). Theoretical studies have shown

Scheme 3. Propargyl-Like (Left) And Allene-Like (Right) Resonance Structures of Nitrile Ylides

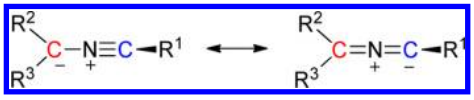

that simple nitrile ylides (for example, R^1 = Me, R^2 = H, Cl, R^3 = H, Cl; Scheme 3) have allene-like character.[36,49] Indeed, the detailed experimental work of the Pimentel group on the IR spectra of nitrile ylides generated from photolysis of 3-phenyl-2*H*-azirine (and their ^{13}C, ^{15}N, and ^{2}H isotopically substituted derivatives) in an N_2 matrix at 12 K led to the proposal of an allene-like rather than a propargyl-like structure.[40] The IR band of the antisymmetric CNC vibration of phenyl nitrile ylide (R^1 = Ph, R_2 = R_3 = H; Scheme 3) was observed in that study as a multiplet feature with main maxima at 1926 and 1903 cm^{-1}. However, in clear contrast, the nitrile ylide derived from the photochemistry of isoxazole **1** in the present study exhibited an absorption at a much higher frequency: i.e., at 2037 cm^{-1} (see Figure 5). In both of the above cases, the experimentally observed frequencies were in excellent accord with theoretical calculations.

Figure 7 presents the experimental infrared data on matrix-isolated nitrile ylides, available from different sources,[50,51] juxtaposed with theoretical calculations carried out at the B3LYP/6-311++G(d,p) theory level. As can be seen, the ν_{as}(CNC) vibration may appear in a very broad frequency range, and its position in the spectrum correlates with the difference between the two "NC" bond lengths (CN ylide and NC nitrile) and therefore with the structure of the nitrile ylide. In the unsubstituted nitrile ylide **7** (▲, |CN| = 127.8 pm and |NC| = 121.9 pm) and phenyl nitrile ylide **8** (■, |CN| = 128.0 pm and |NC| = 122.0 pm) this difference is the smallest (ca. 6 pm) and the ν_{as}(CNC) frequency is the lowest (ca. 1920 cm^{-1}). In the acetyl-substituted nitrile ylide (*anti*-**4** in the

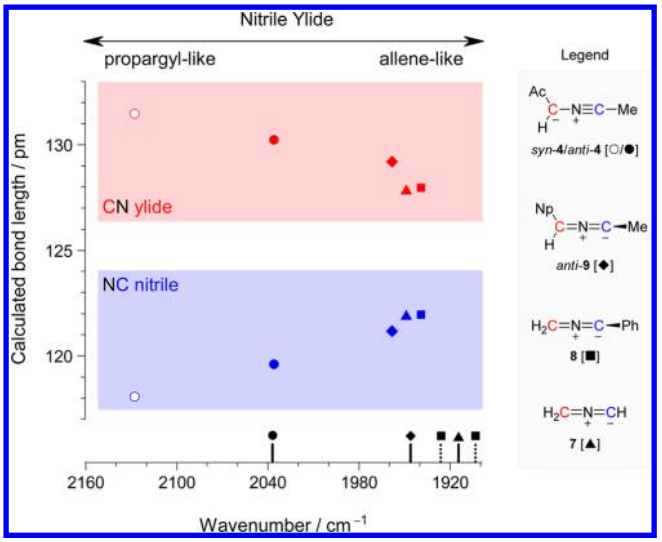

Figure 7. Experimentally observed (bottom, black; **7** (▲),[41] **8** (■),[40] *anti*-**9** (◆),[29] and *anti*-**4** (●; present work)) and theoretically calculated (top, red and blue) frequencies of the ν_{as}(CNC) vibration in nitrile ylides. All theoretical frequencies were obtained for geometries fully optimized at the B3LYP/6-311++G(d,p) level of theory and scaled by 0.980. The equilibrium CN ylide (red) and NC nitrile (blue) calculated bond lengths are shown as functions of the calculated ν_{as}(CNC) frequency. Note that *syn*-**4** (○) does not have an experimental counterpart, as explained in the text. The phenyl nitrile ylide **8** (■, dashed lines) appears in the experiment as a split band due to the Fermi resonance.[40] Abbreviations: Np, 1-naphthyl; Ac, acetyl.

present work, ●, |CN| = 130.2 pm and |NC| = 119.6 pm) this difference is more than 10 pm and the ν_{as}(CNC) frequency is the highest. In other terms, a small difference between the two "NC" bonds means that both of them tend to adopt the double-bond character (allene-like structure), while a greater separation in bond lengths indicates a trend toward the propargyl-like structure.[52] The fact that the nitrile ylide trapped in this work stands apart from other nitrile ylides should be explained due to the presence of the electron-withdrawing substituent (the acetyl group) at the ylide side of the molecule, which promotes a more propargyl-like structure.

■ CONCLUSION

Monomers of 3,5-dimethylisoxazole (**1**) were isolated in argon matrices at 15 K and characterized spectroscopically. Photolysis of **1** at λ = 222 nm yields two primary photoproducts, 2-acetyl-3-methyl-2*H*-azirine (**3**) and 3-acetyl-*N*-methylketenimine (**6**). Most probably, they are formed through a common acetyl vinyl nitrene intermediate **2**. Upon longer times UV irradiation at λ = 222 nm, two additional photoproducts are formed, being subsequently identified as acetyl nitrile ylide **4** and 2,5-dimethyloxazole (**5**).

The unequivocal spectroscopic identification of **3** and **5** generated from **1** was made possible by comparison with infrared spectra of authentic matrix-isolated **3** and **5** obtained in separate experiments. The identification of **4** and **6** was achieved in additional photochemical experiments with UV irradiation at longer wavelengths, where **1** does not react. In particular, ketenimine **6** undergoes syn−anti isomerization on irradiation with λ = 260 nm, while the nitrile ylide **4** transforms into the oxazole **5** by irradiation at λ = 340 nm.

The kinetic data indicate that the elusive carbonyl nitrile ylide reactive intermediate **4** is formed from 2*H*-azirine **3**,

dx.doi.org/10.1021/jo4015672 | J. Org. Chem. 2013, 78, 10657−10665

during the isoxazole−oxazole photochemical conversion. The nitrile ylide **4** can adopt two conformations. The *syn*-**4** conformer has the proper geometry for 1,5-electrocyclization to the oxazole **5** and could not be experimentally detected. In contrast, the nitrile ylide *anti*-**4** conformer is not properly aligned regarding cyclization toward the oxazole **5**, which allowed its experimental capture in the cryogenic matrix and spectroscopic characterization. Interestingly, the nitrile ylide observed in this study, for the first time, stands apart from the few other nitrile ylides reported experimentally, exhibiting a trend toward a propargyl-like geometry instead of an allene-type structure.

EXPERIMENTAL SECTION

Sample. A commercial sample of 3,5-dimethylisoxazole (**1**; 98%) was used. The synthesis of 2-acetyl-3-methyl-2*H*-azirine (**3**) and 2,5-dimethyloxazole (**5**), and experimental IR spectra of these species isolated in argon matrices, are reported in ref 25.

Matrix-Isolation FTIR Spectroscopy. Prior to use, the sample was degassed by the standard freeze−pump−thaw method. Afterward, the sample vapor was premixed with high-purity argon (N60) in a ratio of ∼1:1500, in a 3 L glass reservoir. The premixed sample was then deposited effusively onto a CsI window, cooled to 15 K. A closed-cycle helium refrigeration system was used. The temperature of the CsI window was measured directly by a silicon diode sensor connected to a digital controller, providing stabilization with accuracy of ±0.1 K.

The IR spectra, in the 4000−400 cm^{-1} range, were obtained using a Fourier transform infrared spectrometer, equipped with a deuterated triglycine sulfate (DTGS) detector and a Ge/KBr beam splitter, with 0.5 cm^{-1} resolution. To avoid interference from atmospheric H_2O and CO_2, the optical path of the spectrometer was continuously purged by a stream of dry air.

UV-Laser Irradiation Experiments. The matrices were irradiated through a quartz window of the cryostat, using a frequency-doubled signal beam provided by an optical parametric oscillator (fwhm ∼0.2 cm^{-1}) pumped with a pulsed Nd:YAG laser (repetition rate 10 Hz, pulse energy ∼0.5 mJ, duration 10 ns).

Theoretical Calculations. All calculations were carried out using the GAUSSIAN 09 program package.[53] With the aim of modeling the IR spectra, the geometry optimizations at the B3LYP/6-311++G(d,p) level were followed by harmonic frequency calculations at the same level of theory. To correct for the vibrational anharmonicity, basis set truncation, and the neglected part of electron correlation, the calculated frequencies were scaled by 0.980. The resulting frequencies, together with the calculated intensities, were used to simulate the spectra by convoluting each peak with a Lorentzian function with a full width at half-maximum (fwhm) of 2 cm^{-1}.[54] The peak intensities of the simulated spectra (in arbitrary units of "relative intensity") are several times less than the calculated intensities (in km mol^{-1}).

ASSOCIATED CONTENT

Supporting Information

Tables and figures giving the experimental and calculated IR spectra for 3,5-dimethylisoxazole (**1**), 2-acetyl-3-methyl-2*H*-azirine (**3**), 3-acetyl-*N*-methylketenimine (**6**), and 2,5-dimethyloxazole (**5**), the definition of internal coordinates used in the normal-mode analysis of **1**, least-squares linear fit data of the experimental versus calculated frequencies in the fingerprint region of the IR spectrum of **1**, experimental IR spectra showing the progress from 0 to 180 s of the photochemistry of **1** at λ = 222 nm, calculated relaxed potential energy profiles for the internal rotation of the C−C bonds of **3** and **6**, a comparison of calculated IR spectra of nitrile ylide, *syn*-**4** and *anti*-**4**, with experimental data, most significant resonance structures and IR absorptions for five "non-classic" nitrile ylides, and Cartesian coordinates and frequencies (**1** and **3**−**9**) from B3LYP/6-311++G(d,p) calculations. This material is available free of charge via the Internet at http://pubs.acs.org.

AUTHOR INFORMATION

Corresponding Authors

*E-mail for C.M.N.: cmnunes@qui.uc.pt.
*E-mail for I.R.: reva@qui.uc.pt.

Notes

The authors declare no competing financial interest.

ACKNOWLEDGMENTS

These studies were partially funded by the Portuguese "Fundação para a Ciência e a Tecnologia" (FCT), FEDER, and projects PTDC/QUI-QUI/111879/2009, PTDC/QUI-QUI/118078/2010, FCOMP-01-0124-FEDER-021082, co-funded by QREN-COMPETE-UE. C.M.N. acknowledges the FCT for the Postdoc Grant No. SFRH/BPD/86021/2012.

REFERENCES

(1) *Comprehensive Heterocyclic Chemistry*; Lang, S. A., Lin, Y. I., Eds.; Pergamon: Oxford, U.K., 1984; Vol. *6*, Part 4B.
(2) *Chemistry of Heterocyclic Compounds*; Grünanger, P., Vita-Finzi, P., Eds.; Wiley: New York, 1991; Vol. *49*, Part 1.
(3) Pinho e Melo, T. M. V. D. *Curr. Org. Chem.* **2005**, *9*, 925.
(4) Ullman, E. F.; Singh, B. *J. Am. Chem. Soc.* **1966**, *88*, 1844.
(5) Singh, B.; Ullman, E. F. *J. Am. Chem. Soc.* **1967**, *89*, 6911.
(6) Singh, B.; Zweig, A.; Gallivan, J. B. *J. Am. Chem. Soc.* **1972**, *94*, 1199.
(7) Kurtz, D. W.; Shechter, H. *Chem. Commun.* **1966**, *6*, 689.
(8) Good, R. H.; Jones, G. *J. Chem. Soc. C* **1971**, 1196.
(9) Ferris, J. P.; Antonucci, F. R.; Trimmer, R. W. *J. Am. Chem. Soc.* **1973**, *95*, 919.
(10) Sato, T.; Yamamoto, K.; Fukui, K. *Chem. Lett.* **1973**, 111.
(11) Sato, T.; Saito, K. *J. Chem. Soc., Chem. Commun.* **1974**, *99*, 781.
(12) Padwa, A.; Chen, E.; Ku, A. *J. Am. Chem. Soc.* **1975**, *97*, 6484.
(13) Murature, D. A.; Peres, J. D.; Bertorello, M. M.; Bertorello, H. E. *An. Asoc. Quim. Argent.* **1976**, *64*, 337.
(14) Dietliker, K.; Gilgen, P.; Heimgartner, H.; Schmid, H. *Helv. Chim. Acta* **1976**, *59*, 2074.
(15) Ferris, J. P.; Trimmer, R. W. *J. Org. Chem.* **1976**, *41*, 13.
(16) Sato, T.; Yamamoto, K.; Fukui, K.; Saito, K.; Hayakawa, K.; Yoshiie, S. *J. Chem. Soc., Perkin Trans. 1* **1976**, 783.
(17) Sauers, R. R.; Van Arnum, S. D. *Tetrahedron Lett.* **1987**, *28*, 5797.
(18) Sauers, R. R.; Hadel, L. M.; Scimone, A. A.; Stevenson, T. A. *J. Org. Chem.* **1990**, *55*, 4011.
(19) D'Auria, M. *Adv. Heterocycl. Chem.* **2001**, *79*, 41.
(20) Fonseca, S. M.; Burrows, H. D.; Nunes, C. M.; Pinho e Melo, T. M. V. D.; Rocha Gonsalves, A. M. d. *Chem. Phys. Lett.* **2005**, *414*, 98.
(21) Pavlik, J. W.; St. Martin, H.; Lambert, K. A.; Lowell, J. A.; Tsefrikas, V. M.; Eddins, C. K.; Kebede, N. *J. Heterocyl. Chem.* **2005**, *42*, 273.
(22) Fonseca, S. M.; Burrows, H. D.; Nunes, C. M.; Pinho e Melo, T. M. V. D. *Chem. Phys. Lett.* **2009**, *474*, 84.
(23) Lopes, S.; Nunes, C. M.; Gómez-Zavaglia, A.; Pinho e Melo, T. M. V. D.; Fausto, R. *J. Phys. Chem. A* **2011**, *115*, 1199.
(24) Tanaka, H.; Osamura, Y.; Matsushita, T.; Nishimoto, K. *Bull. Chem. Soc. Jpn.* **1981**, *54*, 1293.
(25) Nunes, C. M.; Reva, I.; Pinho e Melo, T. M. V. D.; Fausto, R.; Šolomek, T.; Bally, T. *J. Am. Chem. Soc.* **2011**, *133*, 18911.
(26) Some experimental evidence (not unequivocal) of vinyl nitrenes **II** and nitrile ylides **IV** have been respectively reported in: (a) Rajam, S.; Murthy, R. S.; Jadhav, A. V; Li, Q.; Keller, C.; Carra, C.; Pace, T. C. S.; Bohne, C.; Ault, B. S.; Gudmundsdottir, A. D. *J. Org. Chem.* **2011**, *76*, 9934. (b) Ref 23.
(27) Nunes, C. M.; Reva, I.; Pinho e Melo, T. M. V. D.; Fausto, R. *J. Org. Chem.* **2012**, *77*, 8723.

(28) Michaut, X.; Vasserot, A.-M.; Abouaf-Marguin, L. *Vib. Spectrosc.* **2004**, *34*, 83.
(29) Inui, H.; Murata, S. *J. Am. Chem. Soc.* **2005**, *127*, 2628.
(30) It is known that nitrogen matrices may increase lifetimes of metastable higher-energy species; see for example: (a) Lopes, S.; Domanskaya, A. V; Fausto, R.; Räsänen, M.; Khriachtchev, L. *J. Chem. Phys.* **2010**, *133*, 144507. (b) Nunes, C. M.; Lapinski, L.; Fausto, R.; Reva, I. *J. Chem. Phys.* **2013**, *138*, 125101.
(31) Lundell, J.; Krajewska, M.; Räsänen, M. *J. Phys. Chem. A* **1998**, *102*, 6643.
(32) Kuş, N.; Sharma, A.; Reva, I.; Lapinski, L.; Fausto, R. *J. Chem. Phys.* **2012**, *136*, 144509.
(33) Lapinski, L.; Rostkowska, H.; Reva, I.; Fausto, R.; Nowak, M. J. *J. Phys. Chem. A* **2010**, *114*, 5588.
(34) Kappe, C. O.; Wong, M. W.; Wentrup, C. *J. Org. Chem.* **1995**, *60*, 1686.
(35) Reva, I.; Nowak, M. J.; Lapinski, L.; Fausto, R. *J. Phys. Chem. B* **2012**, *116*, 5703.
(36) Escolano, C.; Duque, M. D.; Vázquez, S. *Curr. Org. Chem.* **2007**, *11*, 741.
(37) The first direct observation of a nitrile ylide, credited to Schimd et al., was achieved in organic rigid matrices at −185 °C by means of UV spectroscopy. See: Sieber, W.; Gilgen, P.; Chaloupka, S.; Hansen, H.-J.; Schmid, H. *Helv. Chim. Acta* **1973**, *56*, 1679.
(38) Note that relevant information on nitrile ylide intermediates have also been obtained by time-resolved spectroscopy. See ref 36 and references cited therein.
(39) Wentrup, C.; Fischer, S.; Berstermann, H.-M.; Kuzaj, M.; Lüerssen, H.; Burger, K. *Angew. Chem., Int. Ed. Engl.* **1986**, *25*, 85.
(40) Orton, E.; Collins, S. T.; Pimentel, G. C. *J. Phys. Chem.* **1986**, *90*, 6139.
(41) Maier, G.; Schmidt, C.; Reisenauer, H. P.; Endlein, E.; Becker, D.; Eckwert, J.; Hess, B. A.; Schaad, L. J. *Chem. Ber.* **1993**, *126*, 2337.
(42) Naito, I.; Nakamura, K.; Kumagai, T.; Oku, A.; Hori, K.; Matsuda, K.; Iwamura, H. *J. Phys. Chem. A* **1999**, *103*, 8187.
(43) Bednarek, P.; Wentrup, C. *J. Am. Chem. Soc.* **2003**, *125*, 9083.
(44) We are also aware of, at least, other five nitrile ylides captured in low-temperature matrices. These five nitrile ylides, labeled here as "non-classic",[51] were generated as intermediates in the sequence of ring-opening reactions of fused-aromatic nitrenes. See: (a) Kvaskoff, D.; Mitschke, U.; Addicott, C.; Finnerty, J.; Bednarek, P.; Wentrup, C. *Aust. J. Chem.* **2009**, *62*, 275. (b) Addicott, C.; Lüerssen, H.; Kuzaj, M.; Kvaskoff, D.; Wentrup, C. *J. Phys. Org. Chem.* **2011**, *24*, 999. (c) Kvaskoff, D.; Vosswinkel, M.; Wentrup, C. *J. Am. Chem. Soc.* **2011**, *133*, 5413. (d) Wentrup, C.; Lan, N. M.; Lukosch, A.; Bednarek, P.; Kvaskoff, D. *Beilstein J. Org. Chem.* **2013**, *9*, 743.
(45) Fabian, W.; Kappe, C.; Bakulev, V. *J. Org. Chem.* **2000**, *65*, 47.
(46) Two different conformers of a "non-classic" nitrile ylide were observed as a result of a photoinduced ring-opening reaction of a cyclic carbodiimide.[44c] This could suggest photoisomerization in the nitrile ylide.
(47) Reva, I. D.; Lopes Jesus, A. J.; Rosado, M. T. S.; Fausto, R.; Eusébio, M. E. S.; Redinha, J. S. *Phys. Chem. Chem. Phys.* **2006**, *8*, 5339.
(48) Lopes Jesus, A. J.; Rosado, M. T. S.; Reva, I.; Fausto, R.; Eusébio, M. E. S.; Redinha, J. S. *J. Phys. Chem. A* **2008**, *112*, 4669.
(49) Pliego, J. P., Jr. *Chem. Phys. Lett.* **2000**, 142.
(50) Note that we opted not to add to Figure 7 the data for three nitrile ylides reported in refs 39 and 43, due to the following reasons. (i) In ref 39, a bis(trifluoromethyl)-*tert*-butyl nitrile ylide was charaterized by the infrared band ν_{as}(CNC) at 2250 cm^{-1}. We optimized its geometry at the B3LYP/6-311++G(d,p) level, the same as in the present study, and ran the vibrational calculations. The calculated ν_{as}(CNC) frequency (ca. 2097 cm^{-1}, scaled) shows a very significant discrepancy from experiment. This discrepancy must result from the environmental effects on the structure of bis(trifluoromethyl)-*tert*-butyl nitrile ylide generated in a neat KBr pellet at −196 °C. Thus, this result is not directly comparable with IR data on monomeric nitrile ylides isolated in inert (noble gas or nitrogen) matrices. (ii) In the work of Bednarek and Wentrup (**BW**),[43] conjugated nitrile ylides, of the X≡CHCH═C(HCNCH) type, were generated under conditions comparable to those in the present work (in cryogenic noble gas matrices). These nitrile ylides were charaterized by the infrared ν_{as}(CNC) bands at 1930 cm^{-1} (for X = CH, **BW1**), and at 1961/1947 cm^{-1} (for X = N, **BW2**). However, nitrile ylides **BW1** and **BW2** reported in ref 43 could assume at least four different conformations, and indeed more than one rotamer was observed for **BW2**. The ring-contraction reaction has a low predicted barrier for syn−syn conformers (only 3.5 kcal mol^{-1}) and it must occur easily, similarly as it was found in the present study for *syn*-**4**. Therefore, we believe that the observed nitrile ylides must adopt one of the three remaining conformations, with at least one of the dihedrals being anti. According to our B3LYP/6-311++G(d,p) calculations, the different conformers of **BW1** and **BW2** present a significative scattering in the predicted ν_{as}(CNC) frequencies as well as variance in the two "NC" bond lengths. Despite the fact that their precise conformational assignment leaves doubts, **BW1** and **BW2** must belong to the group of the allene-like nitrile ylides, according to their observed ν_{as}(CNC) frequencies.
(51) Note also that Figure 7 does not include the data of five nitrile ylides captured in low-temperature matrices in the sequence of ring-opening reactions of fused-aromatic nitrenes.[44] One of the reviewers of this work pointed out, concerning the IR frequency ν_{as}(CNC) vibration of nitrile ylides, that two more regions characteristic of fully propargylic (up to 2300 cm^{-1}) and carbenic (below 1900 cm^{-1}) structures should be explored. Indeed, some of the nitrile ylide species listed in ref 44 are reported to have IR absorptions near 2200 cm^{-1}. Nevertheless, in these reported structures, the sp^2 carbon atom of the CNC nitrile ylide fragment is inserted in a six-membered ring, which in some resonance structures can be fully aromatic (such as dipolar species marked gray in Figure S7 (Supporting Information)). If this type of resonance structure describes better the structure of the species in question, they cannot be regarded as "classic" nitrile ylide species, and then they cannot be directly comparable with those shown in Figure 7.
(52) A larger separation in the two "NC" bond lengths (|CN| = 138.9 pm and |NC| = 113.1 pm) was observed in an exceptionally stable nitrile ylide, which presents a propargylic structure, by X-ray crystallography. See: Janulis, E. P.; Wilson, S. R.; Arduengo, A. J. *Tetrahedron Lett.* **1984**, *25*, 405.
(53) Frisch, M. J.; Trucks, G. W.; Schlegel, H. B.; Scuseria, G. E.; Robb, M. A.; Cheeseman, J. R.; Scalmani, G.; Barone, V.; Mennucci, B.; Petersson, G. A.; Nakatsuji, H.; Caricato, M.; Li, X.; Hratchian, H. P.; Izmaylov, A. F.; Bloino, J.; Zheng, G.; Sonnenberg, J. L.; Hada, M.; Ehara, M.; Toyota, K.; Fukuda, R.; Hasegawa, J.; Ishida, M.; Nakajima, T.; Honda, Y.; Kitao, O.; Nakai, H.; Vreven, T.; Montgomery, J. A.,Jr.; Peralta, J. E.; Ogliaro, F.; Bearpark, M.; Heyd, J. J.; Brothers, E.; Kudin, K. N.; Staroverov, V. N.; Kobayashi, R.; Normand, J.; Raghavachari, K.; Rendell, A.; Burant, J. C.; Iyengar, S. S.; Tomasi, J.; Cossi, M.; Rega, N.; Millam, J. M.; Klene, M.; Knox, J. E.; Cross, J. B.; Bakken, V.; Adamo, C.; Jaramillo, J.; Gomperts, R.; Stratmann, R. E.; Yazyev, O.; Austin, A. J.; Cammi, R.; Pomelli, C.; Ochterski, J. W.; Martin, R. L.; Morokuma, K.; Zakrzewski, V. G.; Voth, G. A.; Salvador, P.; Dannenberg, J. J.; Dapprich, S.; Daniels, A. D.; Farkas, Ö.; Foresman, J. B.; Ortiz, J. V.; Cioslowski, J.; Fox, D. J. *Gaussian 09, Revision A.2*; Gaussian, Inc., Wallingford, CT, 2009.
(54) Irikura, K. K. *Program SYNSPEC*; National Institute of Standards and Technology, Gaithersburg, MD 20899, USA.